Contents lists available at ScienceDirect

Powder Technology

journal homepage: www.journals.elsevier.com/powder-technology





Systematic study to improve the powder feeding performance and reducing the percentage of fines in roller compactor

Yang S. Mohamad ^{a,*}, Mingzhe Yu ^a, Manfred Felder ^b, Vincent Meunier ^c, James Litster ^a, Agba D. Salman ^a

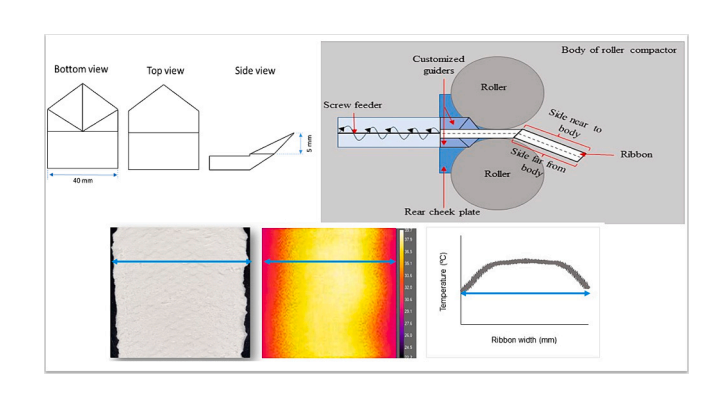
- ^a Department of Chemical and Biological Engineering, University of Sheffield, Mappin Street, Sheffield S1 3JD, UK
- ^b Alexanderwerk GmbH, Remscheid, North Rhine-Westphalia, Germany
- ^c Nestle Research, 1000 Lausanne, Switzerland

HIGHLIGHTS

A systematic study of 14 customized guiders on powder distribution in roller compaction was conducted using PAT.

- Crystalline and spray-dried lactose with varying flowability were utilized.
- Powder with low flowability shows nonuniform distribution during compaction.
- Customized guiders improved temperature distribution, uniformity, and reduced fines in low-flowability lactose powder.

GRAPHICAL ABSTRACT



ARTICLE INFO

Keywords:
Roller compaction
Ribbon uniformity
Customized guider
Temperature
Fines

ABSTRACT

Roller compaction is a widely used continuous dry granulation process in the food and pharmaceutical industries. The flow and distribution of the powder across the rollers in the compaction area plays a crucial role in determining the quality of the final product. Non-uniform powder flow and distribution across the rollers can lead to variations in quality across the ribbon, resulting in uneven qualities in the granules. Hence, it is essential to enhance the powder flow and distribution across the rollers in the compaction area. Besides that, insufficient compaction stress on both sides of the roller edges can also contribute to presence of uncompacted fines during compaction process.

This research aims to systematically study a whole range of customized guiders design (T-1 until T-14) that improves powder flow and distribution across the rollers and reduces the percentage of fines in the compaction zone. The 3D printed customized guiders with different grade (1 mm until 14 mm) were applied in roller compactor with horizontal feeding system to control the amount of powder passing through the roller width by guiding more powder to the sides between the rollers and less powder to the centre. The effectiveness of the design was validated by examining crystalline and spray dry lactose powders with varying flowabilities using online thermal imaging. The results demonstrate a significant trend, indicating improved uniformity of powder flow and distribution across the rollers and reduced production of fines. These findings have the potential to

E-mail address: ysbmohamad1@sheffield.ac.uk (Y.S. Mohamad).

^{*} Corresponding author.

1. Introduction

Agglomeration is a size-enlargement technique commonly employed in industries such as food and pharmaceuticals to improve the flowability and uniformity of final product by bonding them together into larger entities. The strength of these agglomerates is crucial for effective transportation to end consumers. Roller compaction is one of the most widely used dry agglomeration processes, which eliminates the need for a separate drying stage and reducing energy consumption. In this process, particles are bonded together through compaction forces without the addition of liquid. Roller compaction is also a continuous process that enhances overall process efficiency and easy for scalability [1–5].

The roller compaction process consists of three important stages: feeding, compaction, and crushing. In the horizontal feeding stage, powder particles undergo rearrangement under low pressure before entering the compaction stage, where they are compressed between two counter-rotating rollers, forming ribbons. These ribbons then enter the crushing stage, where they are milled into granules [6]. The flow and distribution of the powder across the rollers in the compaction area significantly affects the quality of the final product [7–11]. The compaction zone operates in such a way that more powder is fed at the center than at the sides of the rollers, resulting in a higher density of ribbons at the center compared to the sides. Non-uniform powder distribution across the ribbon width affects the uniformity of quality at different locations across the ribbons, ultimately leading to uneven qualities in the granules [2,12–14].

Furthermore, unsatisfactory reduction in the amount of fines (uncompacted powder) leaking under the rollers and side-sealing cheek plates is an issue faced by the pharmaceutical and food industries [7-10,15,16]. Various attempts have been made to overcome this limitation of roller compaction, such as collecting the fines in a small bag and recycling the fines back into the feeding hopper to reduce powder wastage [17-21]. However, it should be noted that fines recycling is only feasible when the fines have the same composition as the primary material. When multiple materials are employed, this recycling method cannot be applied as it would introduce inhomogeneity in the product [19]. Previous experimental works show that the type of materials used and powder flow are possible factors leading to the production of fines in the dry granulation process [20,22,23,24]. Non-uniform powder distribution across the ribbon width, with more powder concentrated at the center than the sides, results in uneven stress distribution across the rollers, affecting the density and strength of the ribbon sides [5]. Weak sections of the ribbon sides contribute to the generation of fines during the compaction process [21]. Reducing the amount of fines produced would benefit industrial applications in terms of long-term sustainability by reducing material recycling and energy consumption during continuous processes. Therefore, improving powder flow and distribution across the rollers in the compaction area is essential to produce better quality ribbons and granules while minimizing fines production.

This study proposes a sustainable method to enhance powder flow and distribution across the rollers and reduce the percentage of fines produced during roller compaction by implementing customized guiders in the compaction zone. Previous research has explored the impact of using a shortlist range of three guiders for each material on powder flow. However, this work presents a systematic study involving a comprehensive range of 14 grades of customized guiders, ranging from 1 mm to 14 mm, applied to crystalline and spray-dry lactose powders with different flowability property. The 3D printed customized guiders were incorporated into the roller compactor to regulate the amount of powder passing through the roller width. This was achieved by directing more powder towards the sides between the rollers and less towards the

center. The primary objective of this research is to conduct a systematic investigation into the effect of customized guiders with different grades on the uniformity of powder flow and distribution across the rollers, as well as the quality of the ribbons produced. The quality of the ribbons will be evaluated based on temperature distribution profiles across the ribbon width, the percentage of fines, and the achieved ribbon width during the roller compaction process.

2. Experimental method

2.1. Primary powder properties

Milled Crystalline Alpha-Lactose Monohydrate (Volac International Ltd., United Kingdom) with grade of 200 M is a type of lactose with crystalline structure was referred to as Volactose. Meanwhile, Super Tab 11SD (DFE Pharma, Germany) is a spray dry lactose with partially amorphous content as obtained from the manufacturer was referred to as 11SD. In the beginning of the experiment, the particle size distribution of the primary powders was measured by the Camsizer XT (Retsch Technology GmbH, Germany) while the flow function coefficient (ffc), angle of wall friction and angle of internal friction were measured by the Ring Shear Testers RST-XS (Dietmar Schulze, Germany) at 20% relative humidity at 20 $^{\circ}\text{C}$ as shown in Table 1. The ffc values of different powders were measured by using 5000 Pa normal load at pre-shear, and normal load at the shear of three different level stress to determine the flowability of the powders. The flow function coefficient (ffc) was used to evaluate the powder flowability where a higher value indicates higher flowability [10].

2.2. Preparation of ribbons

Volactose and 11SD powders were subjected to sieving using British Standard mesh sieve with a maximum size limit of d₉₀ respectively and stored under a relative humidity of 12% for three days to ensure reproducible results as it is well known that amorphous powder such as 11SD are very sensitive to moisture and could therefore be affected by storage conditions [25-28]. The equilibrated powders were then consolidated into ribbons using a roller compactor, specifically the Alexanderwerk WP120 Pharma from Germany. This roller compactor used a horizontal screw feeding system and side cheek plates to prevent powder leakage during compression. A hydraulic pressure of 30, 60 and 100 bar was applied between knurled surface rollers ('diamond pattern surface') to form the ribbon shown in Table 2 [7,9]. Knurled surface rollers used during compaction process has the same pattern, material and design as 'diamond' pattern surface plate used in the ring shear tester for measuring the angle of wall friction. During the ribbon production, a feedback system was employed to maintain a constant 3 mm gap between the rollers by constantly adjusting the feed rate while the roller speed was kept constant at 3 rpm.

2.3. Temperature distribution profiles across ribbon width

An online thermal imaging system (FLIR A655 sc, United States) was used to capture thermal images of the ribbon as it exited the rollers [6]. The thermal camera was positioned opposite to the direction of ribbon exiting from the roller gap in the room temperature of 20 °C [21]. The distance between the thermal camera and the exiting ribbon was 30 cm while the height of thermal camera was the same height as where the ribbon exiting from the roller gap from as shown in Fig. 1. The diameter of the roller width was 40 mm. Fig. 2 (a) shows the image plan view full ribbon exiting from roller compactor while Fig. 2 (b) shows the image of

full ribbon as captured by the thermal camera. The lighter the colour in the image, the higher the temperature of the ribbon which was shown in the colour- temperature scale. The high temperature usually indicates high stress acting on the the ribbon while the low temperature shown the low stress on the ribbon as shown in Fig. 2 (c) [21].

2.4. Relative temperature uniformity

The relative temperature uniformity (RTU) was defined using Eq. (1) as shown in Fig. 3.

Relative temperature uniformity =
$$(L/RW) \times 100\%$$
 (1)

L is defined as the response length, measured from the point of maximum temperature to the furthest point on the ribbon where the temperature is relatively uniform on both sides. A relatively uniform temperature is considered to be any temperature within the error range (\pm δ Temp) from the maximum ribbon temperature [10,29]; where, RW was the complete ribbon width when ribbons exit roller gap.

Deviation of temperature (δ) was defined as a default maximum range index for general determination of uniformity range, different materials need to use individual range ratio to identify their own relative uniform temperature (ribbon temperature of different materials varied differently in the process) as shown in Eq. (2). Any measuring temperature \pm error bar within the deviation range, could be defined as relative uniform temperature.

$$\delta \text{Temp} = (\text{Tcentre} - \text{Tedge})/\text{Taverage}$$
 (2)

Tcentre = Temperature of the ribbon at the centre.

Tedge = Temperature of the ribbon at the edge away from the temperature at the centre.

 $\label{eq:Taverage} \textbf{Taverage} = \textbf{Average} \ \textbf{temperature} \ \textbf{of} \ \textbf{the} \ \textbf{profile} \ \textbf{across} \ \textbf{the} \ \textbf{ribbon} \\ \textbf{width}.$

Fig. 3 also shows that the ribbon width as divided into two sides The side near to the body of roller compactor (SN) is adjacent to the rear cheek plate while the side far from the body of roller compactor (SF) is closed to the front cheek plate.

2.5. Collection of fines

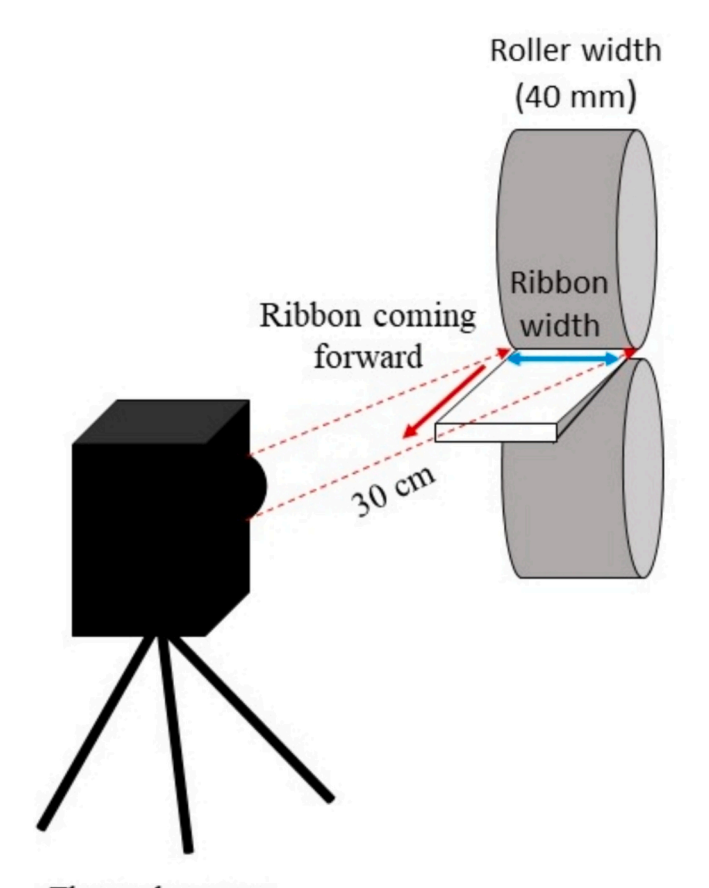
During the roller compaction process, it was ensured that the rollers were thoroughly cleaned, washed and dried between each replication and the temperature of machine was measured to be at the room temperature before the start of the experiment. This practice was implemented to prevent any powder residue from sticking to the rollers, which could potentially compromise the accuracy of the results. In this study, "fines" referred to the weight of un-compacted powder with particle size less than the d_{90} of the primary powder of the material. This was determined by collecting the amount of ribbon, flakes, and fines produced under the compaction zone (under the rollers). Collection was carried out for 1 min after steady state conditions of hydraulic pressure and roller gap were achieved [17,29]. The fines were then separated from the ribbons and flakes using British Standard mesh siever. The percentage of fines produced from compacting Volactose and 11SD powders was calculated.

2.6. Ribbon width

After production, the ribbons were then stored in 20% relative

Table 2The process parameters used for roller compactor.

The parameters	WP 120 Pharma		
Roller pressure (bar)	30, 60 and 100		
Roller speed (rpm)	3		
Roller gap (mm)	3		
Type of guider	Customized guider T-1 until T-14		



Thermal camera

Fig. 1. Schematic diagram of arrangement of thermal camera with the ribbons exiting the roller compactor.

humidities before being characterised. The ribbon width from Volactose and 11SD powders produced using different types of guiders are measured. The average of 10 replications of ribbons width are taken randomly from the collection of ribbon, flakes and fines after the state conditions of hydraulic pressure and roller gap were achieved. The ribbon width was measured using vernier callipers (Magnusson, United Kingdom) with accuracy of ± 0.2 mm. The ribbons collected were made sure to be full width ribbon without any breakage at the sides to avoid inaccuracy of the results.

2.7. Design of customized guider

This study has improved the range of maximum tip of customized

Table 1The primary powder properties.

Materials	Particle size, d ₁₀ (μm)	Particle size, d ₅₀ (μm)	Particle size, d ₉₀ (μm)	Flow function coefficient (ffc)	Angle wall friction (°)	Angle internal friction (°)
Volactose Super Tab 11SD	$\begin{array}{c} 11.6 \pm 1.73 \\ 41.1 \pm 1.06 \end{array}$	$75.6 \pm 1.57 \\ 104.2 \pm 1.85$	$183.3 \pm 1.42 \\ 202.0 \pm 1.23$	$\begin{array}{c} 2.8 \pm 0.08 \\ 20.4 \pm 1.97 \end{array}$	$34.5 \pm 0.50 \\ 24.9 \pm 0.35$	$45.8 \pm 0.45 \\ 33.3 \pm 0.30$

guiders applied which located at the feeding zone between the feeding screw and rollers in the roller compactor as shown in Fig. 4 (front view). The black arrow indicates the direction of unidirectional rotation for the screw feeder, which moves towards the body of the roller compactor and drive the powder to the rollers. The side near to the body of roller compactor is adjacent to the rear cheek plate while the side far from the body of roller compactor is closed to the front cheek plate. The thermal images captured the full width of the ribbon exited from the rollers including the ribbon side near to the body of the roller compactor and ribbon side away from the roller compactor. The guiders (side view) located between the screw feeder and the rollers. These customized guiders were designed with convex surface designs and slope plane at maximum tip grades from 1 mm to 14 mm. The convex surface design aimed to redirect the powder from the centre to the side between the rollers. Fig. 5 showed the examples of customized guiders with a maximum tip grade of 5 mm (T - 5) from bottom, top and side views. Each grade means 1 mm difference for the tip height of customized guiders. The customized guiders are produced using a 3D printer -Ultimaker 3 (Ultimaker, Netherlands) with PLA filament (polylactic acid). A systematic study of 14 guiders as shown in Fig. 6 (top view) was carried out to investigate the effect of customized guiders with different grades on powder flow and distribution across the rollers and the percentage of fines.

3. Results and discussions

The quality of the final product is significantly influenced by the flow and distribution of powder across the rollers within the compaction area. In this zone, the roller compactor operates in such a way that resulted a greater flow of powder at the centre compared to the sides of the rollers, resulting in stronger ribbons at the centre. The difference in strength between the centre and the sides of the ribbon can be observed using dotted lines in Fig. 7 where the two side of the ribbon which are the weaker sides break easily right after the roller compaction process compared to the centre part of the ribbon. The uneven distribution of powder across the ribbon width significantly impacts the consistency of quality at various locations along the ribbons, ultimately causing variations in granule quality. Moreover, the weaker side of the ribbon with lower density contributes to an increased production of fines, along with fines leaking underneath the rollers, as depicted in Fig. 8.

A systematic investigation into the effect of customized guiders with different grades on the uniformity of powder flow and distribution across the rollers and the quality of the ribbons produced is evaluated based on temperature distribution profiles across the ribbon width, percentage of fines, and ribbon width achieved through the roller

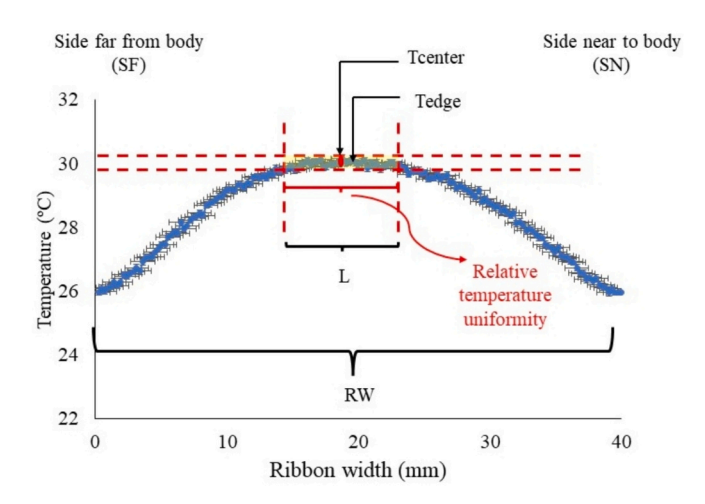


Fig. 3. Method to calculate the relative temperature uniformity.

compaction process. The analysis is carried out on Volactose and 11SD powders with different flow property at different pressure.

3.1. Temperature distribution profiles across the ribbon width using 14 customized guiders

The results in Fig. 9, Fig. 10 and Fig. 11 show the temperature distribution profiles across the ribbon width using T-1 until T-14 customized guiders for Volactose while the results in Fig. 12, Fig. 13 and Fig. 14 show the temperature distribution profiles across the ribbon width using T-1 until T-14 customized guiders for 11SD at 30 bar, 60 bar and 100 bar respectively. The range of temperature was shown using a colour temperature scale where the lowest temperature shows purple colour while the highest temperature shows dark red colour. The high temperature usually indicates high stress and more powder flow as the friction between the powder particles generates heat energy [7–10,17]. The analysis for the 14 guiders in this section will be analysed using colour scale.

Based on Fig. 9, the temperature distribution profile of Volactose ribbons produced using the T-1 and T-14 customized guider at 30 bar revealed higher temperatures at the center (green and blue) than at the sides (purple). Besides that, the application of T-1 and T-2 also shows a higher temperature at the centre compared to the other customized guiders. This trend can be observed when using T-3 to T-14 where a decrease of temperature at the centre can be seen with the changes of colour from green to blue compared to T-1 and T-2 which may indicates

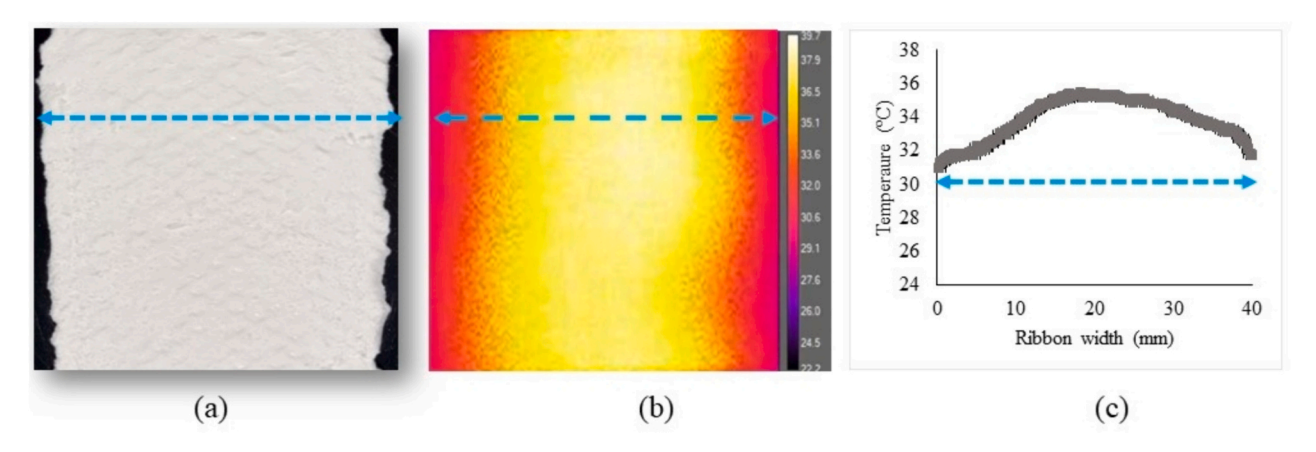


Fig. 2. (a) Plan view of ribbons exiting from the roller compactor with blue line indicates full ribbon width, (b) Image of ribbon as recorded by thermal camera with blue line indicates full ribbon width and (c) analysis of strong and weak parts of the ribbon as indicated by the temperature distribution profile measured by thermal camera with blue line indicates full ribbon width. (For interpretation of the references to colour in this figure legend, the reader is referred to the web version of this article.)

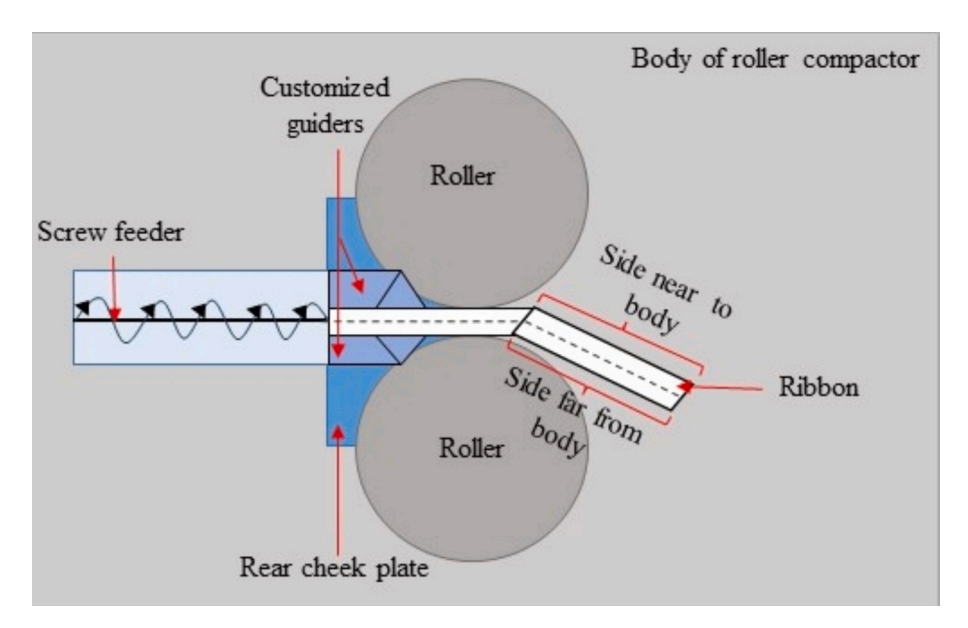


Fig. 4. Front view of feeding screw and rollers. The black arrow indicates the direction of rotation for the screw feeder. The guiders are in side view position located between the screw feeder and the rollers.

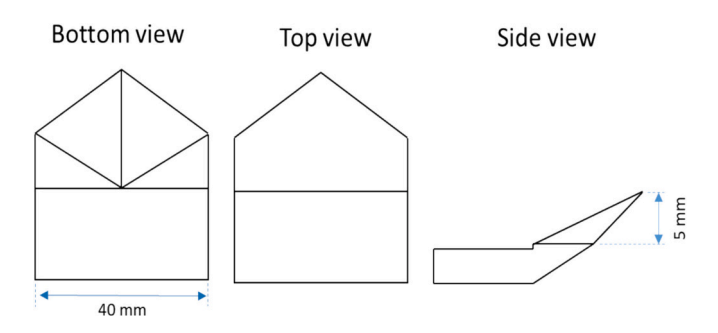


Fig. 5. Example of the customized guider maximum tip grade of 5 mm for T-5 from bottom, top and side views.

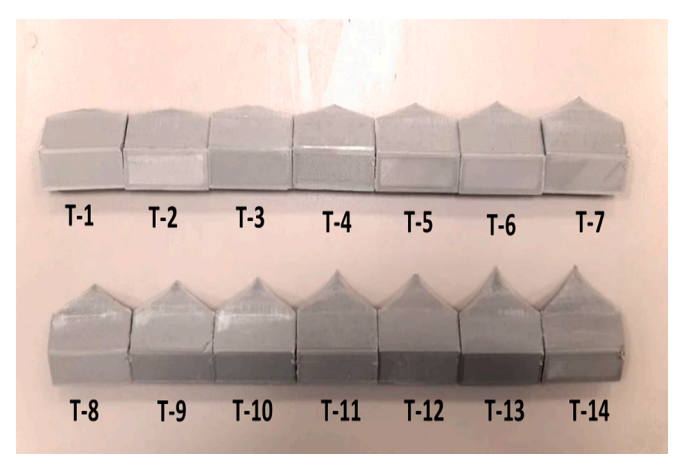


Fig. 6. Customized guiders T-1 until T-14 from top view.

improvement in the uniformity of powders across the ribbon width.

The finding in Fig. 10 for Volactose at 60 bar revealed a high temperature at the center (orange and green) for T-1 to T-14 than at the sides (blue), indicating non-uniform powder distribution across the ribbon width. However, an interesting trend was observed when comparing the temperature at the centre between the 14 customized guiders. Between T-5 to T-13, there was a gradual decrease of temperature at the centre

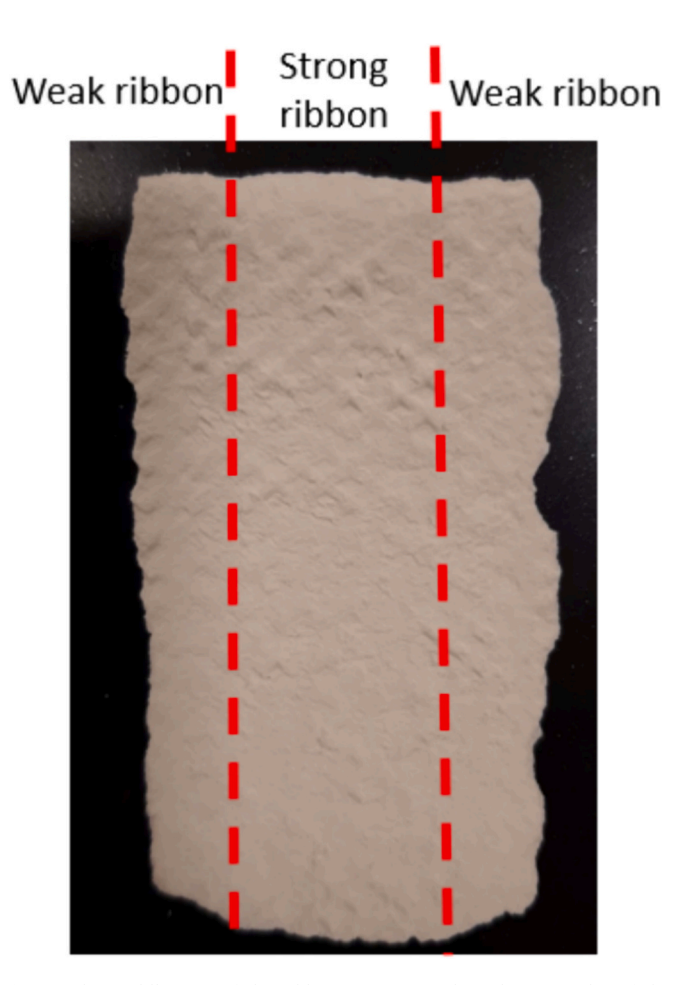
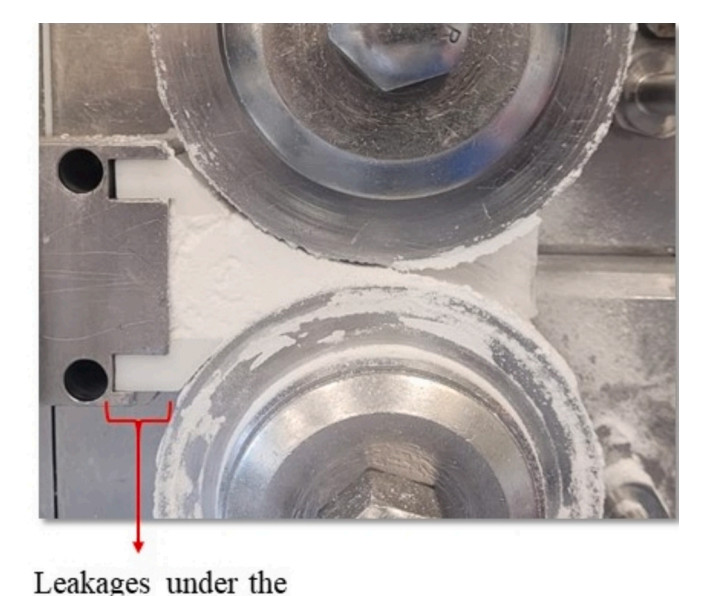


Fig. 7. The middle part of the ribbon is stronger than the two sides of the ribbon as indicated by breakage at the sides.

indicated from the changes of colour from orange to light green. The gradual decrease of temperature at the centre indicates shows improvement in the uniformity of powders across the ribbon width. However, there is a slight increase in temperature at the centre for T-14



rollers

Fig. 8. Leakages of fines under the rollers.

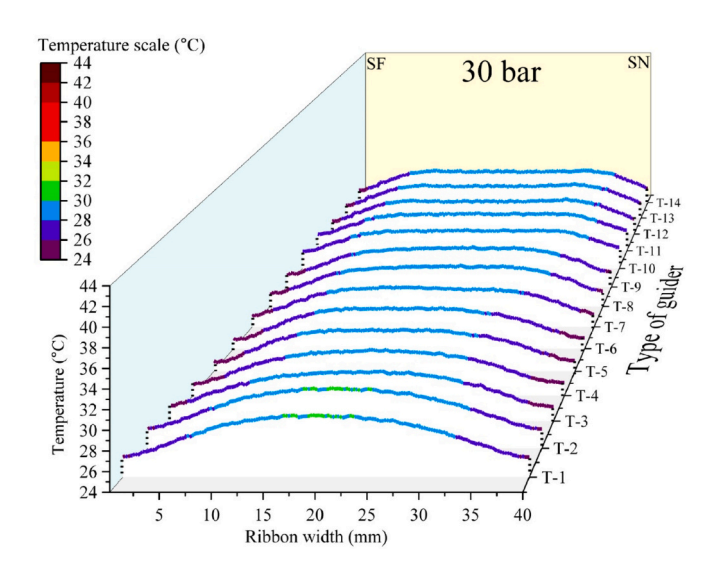


Fig. 9. Temperature distribution profile across the roller width for Volactose powder using customized guider T-1 until T-14 at 30 bar.

to 34.0 $^{\circ}\text{C}$ (orange), indicating a non-uniform distribution of powder across the ribbon width.

Similarly, the result in Fig. 11 for Volactose at 100 bar shows a higher temperature at the centre (red) compared to the sides (blue) for all 14 customized guiders. In addition, a high temperature (dark red) was observed at the center when using T-1 to T-6 compared to other customized guiders. This observation indicates a non-uniform distribution of powder across the ribbon, which attributed to the insufficient dimension grade of these customized guiders to effectively redirect the powder from the center to the sides. A changed of colour at the centre from dark red to light red can be seen with application of T-4 to T-14 showing a decrease of temperature at the centre. This shows that there is an improvement in the temperature distribution profile with application of T-4 to T-14. In addition, In addition, the maximum temperatures at the center for Volactose are higher compared to those at 30 bar and 60 bar, primarily due to the higher compression pressure of 100 bar, which generates more heat energy [21]. The high pressure, coupled with the

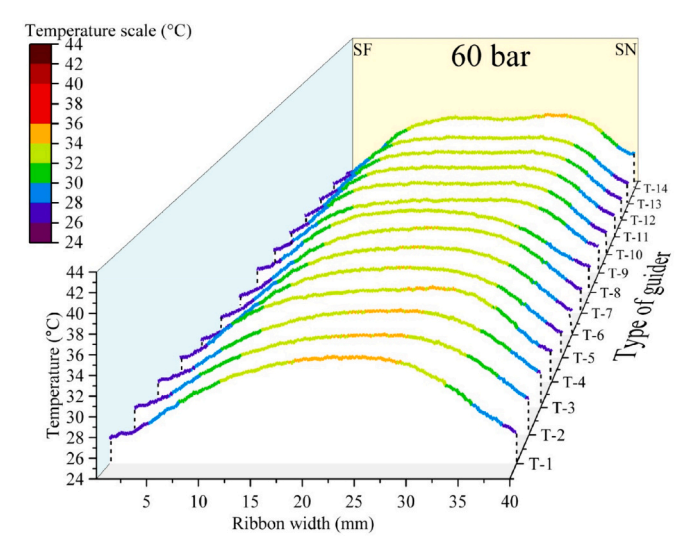


Fig. 10. Temperature distribution profile across the roller width for Volactose powder using customized guider T-1 until T-14 at 60 bar.

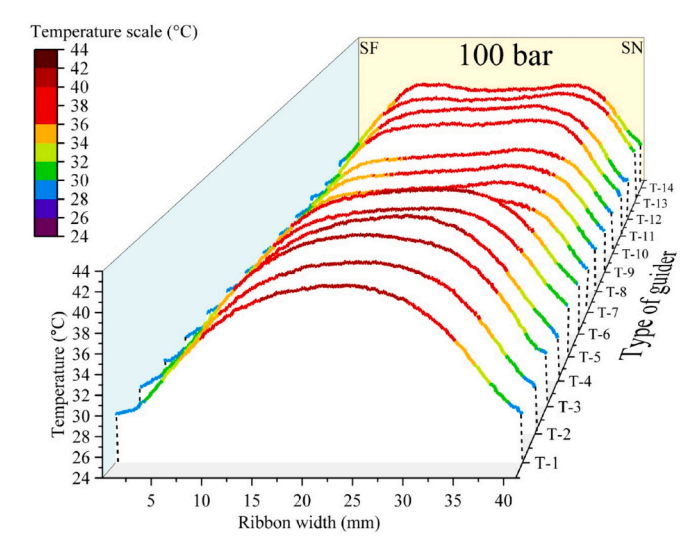


Fig. 11. Temperature distribution profile across the roller width for Volactose powder using customized guider T-1 until T-14 at 100 bar.

longer dimensions of the guiders from T-11 to T-14, could be the reason for the temperature distribution profiles to be higher than those observed from T-8 to T-10.

Based on the results from Fig. 12 for 11SD at 30 bar, the temperature distribution profile of ribbons from 11SD shows a higher temperature (blue) at the centre than at the sides (purple) for customized guiders between T-1 to T-10. However, from T-11 to T-14, the colour at the centre changed to purple showing a decrease in the temperature distribution profile compared to T-1 until T-10. Besides that, T-11 to T-14 also show a lower temperature at the centre than at the sides which could be due to overdirecting of powder at longer dimension of guiders.

The result displayed in Fig. 13 for 11SD at 60 bar indicate a higher temperature at the centre (green and blue) compared to the sides (purple) with application of T-1 until T-12. In contrast, the usage of T-13 to T-14 show a lower temperature at the centre (dark purple) than at the sides (green) showing non-uniform distribution of powder across the ribbon width. In addition, T-1 to T-3 produced a high temperature range at the center (green). The high temperature range can be attributed to non-uniform powder distribution across the ribbon width due to insufficient redirection of powder from the center to the sides Additionally,

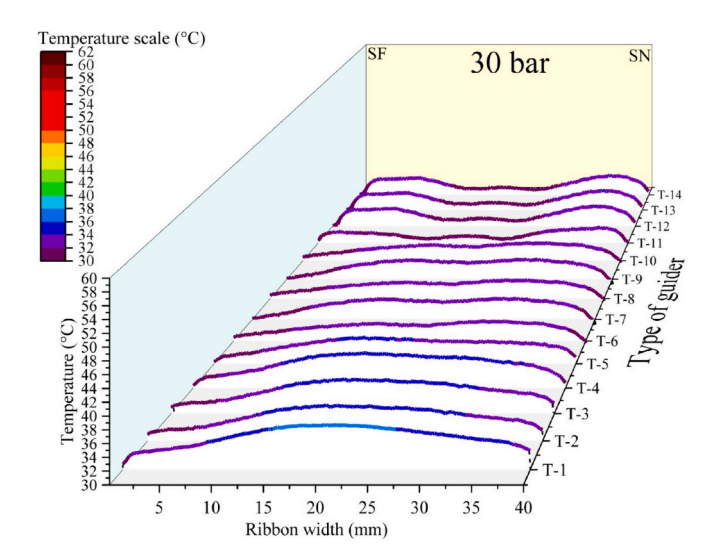


Fig. 12. Temperature distribution profile across the roller width for 11SD powder using customized guider T-1 until T-14 at 30 bar.

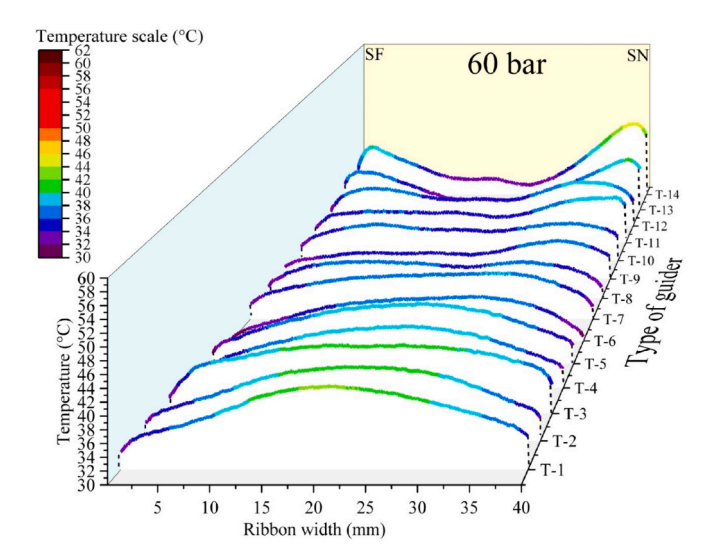


Fig. 13. Temperature distribution profile across the roller width for 11SD powder using customized guider T-1 until T-14 at 60 bar.

the results reveal that the application of T-4 to T-14 show a gradual changed of colour at the centre from blue to purple. The changes of colour at the centre indicates a decrease in temperature distribution profile at the centre compared to T-1 until T-3.

A completely different trend in powder distribution emerged when applying T-1 to T-14 customized guiders on 11SD at 100 bar as shown in Fig. 14. A high temperature distribution profile at the centre (red) was observed at T-1 until T-7 compared to the sides (orange). Furthermore, the colour of maximum temperatures at the centre for 11SD powder at 100 bar was red, showing a higher temperature compared to 11SD powders at 60 bar which is green. This is because 100 bar provides a higher compaction pressure than 60 bar causing more friction of particles to generate more heat energy. Powder temperatures distribution profile for 11SD at 100 bar started to exhibit higher values on one side only compared to the other sides between T-2 and T-7 for customized guiders which could probably resulted from the unidirectional rotation of the screw feeder pushing more powders to one side than the other as reported by other studies [7,30]. Between T-8 and T-14, the powders were excessively redirected to the sides of the cheek plates at 100 bar, resulting in friction between the powder particles and the side cheek

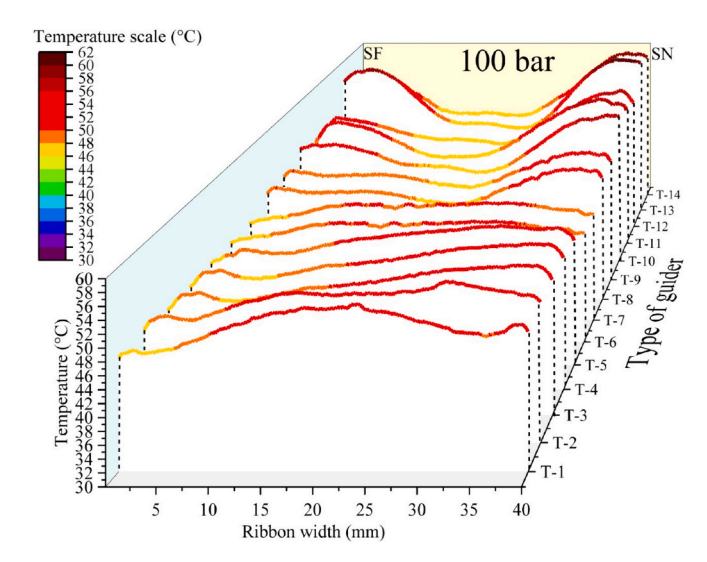


Fig. 14. Temperature distribution profile across the roller width for 11SD powder using customized guider T-1 until T-14 at 100 bar.

plates, and changing the colour at the centre from red to orange. The change of colour at the centre shows a drop of temperature distribution profile at the centre creating non-uniform distribution of powder across the ribbon width.

3.2. Temperature distribution profiles across the ribbon width using selected customized guiders

The results in Fig. 15, Fig. 16, and Fig. 17 show the temperature distribution profiles across the ribbon width using selected customized guiders for Volactose while Fig. 18, Fig. 19, and Fig. 21 display the temperature distribution profiles across the ribbon width using selected customized guiders for 11SD at 30 bar, 60 bar, and 100 bar, respectively. The guiders were selected from a set of 14 customized options based on the one that produced the most significant changes in the temperature distribution profiles across the roller width. The temperature range is represented using a colour temperature scale, where the lowest temperature is indicated by a purple colour and the highest temperature is represented by a dark red colour. Different range of y-axis scale was drawn to capture and analyse the difference in shape, colour and

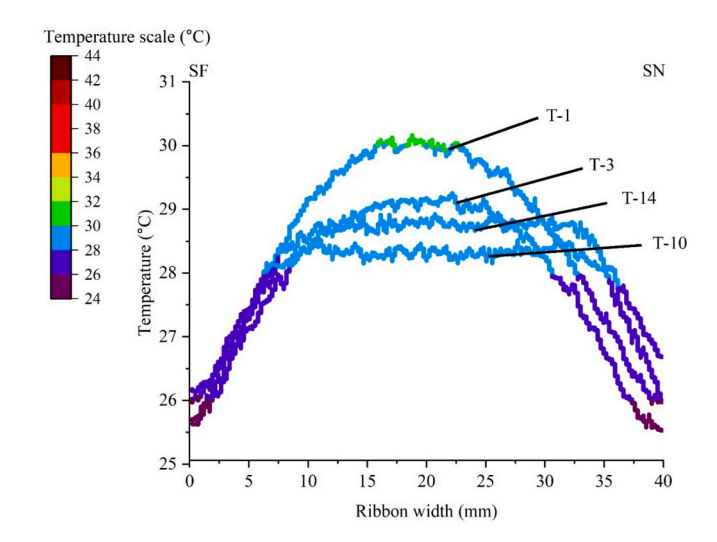


Fig. 15. The temperature distribution profile across the roller width for Volactose powder using selected customized guider at T-1, T-3, T-10 and T-14 at 30 bar.

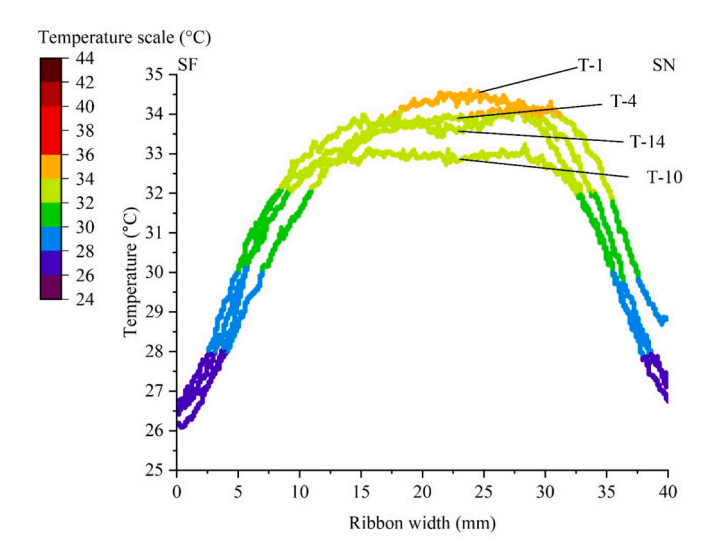


Fig. 16. The temperature distribution profile across the roller width for Volactose powder using selected customized guider at T-1, T-4, T-10 and T-14 at 60 bar.

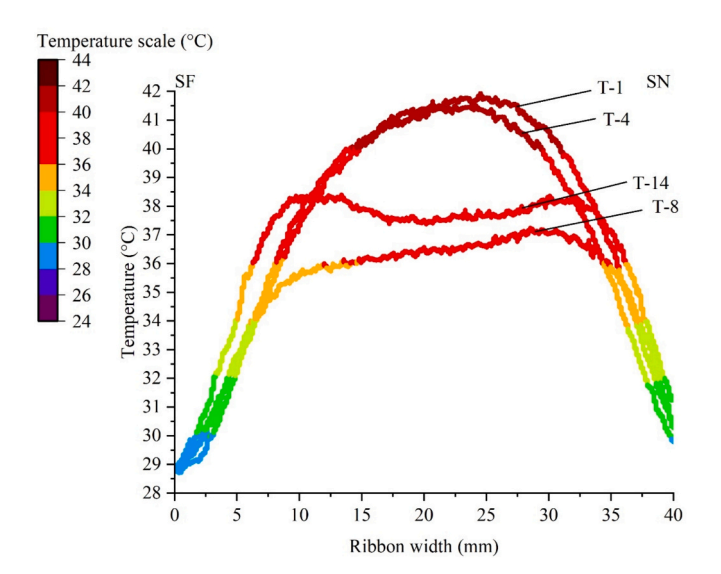


Fig. 17. The temperature distribution profile across the roller width for Volactose powder using selected customized guider at T-1, T-4, T-8 and T-14 at 100 bar.

temperature of the profile across the ribbon width between the selected customized guiders.

The result in Fig. 15 reveals a significant shift in the temperature distribution profile for Volactose at 30 bar when comparing selected customized guiders, namely T-1, T-3, T-10, and T-14. Applying T-1 results in a bell-shaped curve at the centre around 30 °C (dark green). In addition, the temperatures at the far side from the body of roller compactor was observed at 26 °C (dark blue), while those closer to the body reach 27 °C (darks blue), indicating non-uniform powder distribution across the ribbon width. The rise in temperature at the center could be due to the crystalline powders breaking or deforming, creating friction between particles, generating heat energy, and increasing stress at the center. The results for T-3 to T-10 show that the curve at the center gradually flattens, with temperatures dropping to a low of 28 °C (light blue) while both sides stabilize at 25.5 °C (purple) for T-10. The widest flat range in temperature distribution appears in T-14, suggesting the most significant improvement in powder distribution uniformity across the ribbon width compared to other customized guiders. Furthermore,

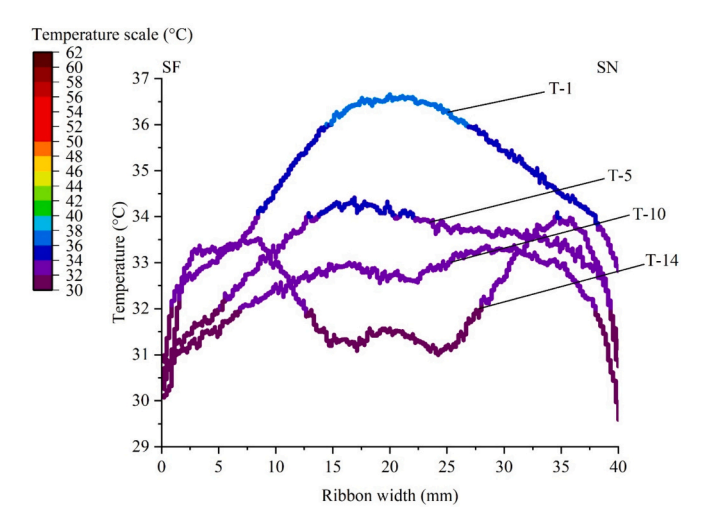


Fig. 18. The temperature distribution profile across the roller width for 11SD powder using selected customized guider at T-1, T-5, T-10 and T14 at 30 bar.

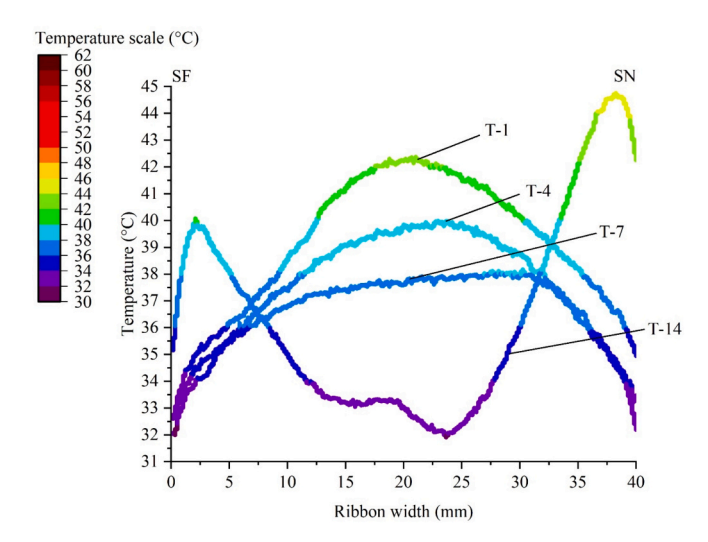


Fig. 19. The temperature distribution profile across the roller width for 11SD powder using selected customized guider at T-1, T-4, T-7 and T-14 at 60 bar.

temperatures near the body of roller compactor are notably higher than those further away, particularly noticeable in T-1 and T-3. This difference likely arises from the unidirectional rotation of the screw feeder towards the body of roller compactor, increasing friction and heat generation between powder particles and the side cheek plates closer to the body. In contrast, both T-10 and T-14 display similar ribbon temperatures on both sides of the body of the roller compactor. These findings imply that customized guiders with dimensions of 14 mm enhance powder distribution across the ribbon width compared to those with dimensions of 1 mm to 3 mm.

The result in Fig. 16 presents a notable shift in the shape of the temperature distribution profile for Volactose at 60 bar, focusing on the usage of selected customized guiders: T-1, T-4, T-10, and T-14. Initially, T-1 exhibits a bell-shaped curve at the centre around 34 $^{\circ}$ C (orange), while temperatures on the far side from the roller compactor reach 26 $^{\circ}$ C (dark blue), and those nearer register at 29 $^{\circ}$ C (light blue). This difference may be resulted from the unidirectional rotation screw feeder towards the body of roller compactor, inducing friction and heat generation between powder particles and the cheek plates near to the equipment's body, compared to the farther side. Subsequently, with the increasing grade of the customized guider, the curve at the center becomes more flattens, particularly evident with T-10, where the

temperature decreases to 32 °C (light green) at the center and stabilizes at around 26 °C (dark blue) on both sides. T-10 displays the widest flat range in the temperature distribution profile, indicating improved uniformity in powder distribution across the ribbon width compared to other customized guiders. In contrast, the application of T-14 raises the center temperature to 34.0 °C (orange), indicating a non-uniform distribution of powder across the ribbon width. The changes observed between T-1 and T-14 in both shape and temperature distribution profile at the center can be attributed to the increased grade of the customized guider, facilitating powder movement from the center towards the sides. This movement enhances friction and heat energy generation between powder particles and the side cheek plates.

An obvious change in the shape of the temperature distribution profile was observed in Fig. 17 for Volactose at 100 bar when comparing the selected customized guiders of T-1, T-4, T-8, and T-14. Initially, both T-1 and T-4 exhibited a bell-shaped curve at the center with temperatures around 42 °C (dark red). However, with the application of T-8, there was an improvement in the flat range of the curve at the center, resulting in a decrease in temperature from 42 °C to 38 °C (medium red). This indicates that T-8, with a maximum tip grade of 8 mm, achieved the most significant improvement in the uniformity of powder distribution across the ribbon width compared to the other customized guiders at 100 bar. However, when T-14 customized guiders were applied, the temperature distribution profile began to exhibit non-uniform powder distribution across the ribbons. This was due to the combined effects of friction energy from excessive redirection of powder by customized guiders with a 14 mm tip to the sides of cheek plates, influenced by the high pressure of 100 bar. It is noteworthy that the temperature on the far side from the roller compactor reached 28.5 °C (light blue), while the one nearer to the equipment was approximately 30.5 °C (light green) for T-1, T-4, T-8, and T-14. These results indicate that even with the improvement of the temperature distribution profile at the center for T-8, there is still a difference in temperature at both sides of the ribbon. This difference can be attributed to the unidirectional rotation of the screw feeder which drove the powder towards the body of the roller compactor at high pressure causing friction with rear side cheek plate resulting in increasing in temperature at the side near the roller compactor than the opposite side.

A noticeable change in the shape of the temperature distribution profile was identified in Fig. 18 for 11SD at 30 bar when examining the impact of the selected customized guiders T-1, T-5, T-10, and T-14. The application of T-1 shows a bell-shaped curve at the center with a temperature around 36 °C (medium blue), while the temperature on the far side of the roller compactor is 30 $^{\circ}$ C (dark purple), and the temperature near the equipment is observed at 33 °C (light purple). The high temperature at the center may be due to the breakage or deformation of amorphous powders, creating friction between the powder particles and generating heat energy. Additionally, the increase in temperature on the side near the roller compactor compared to the side further from the body of the equipment is due to the unidirectional rotation of the screw feeder towards the body of the roller compactor. Subsequently, the shape of the curve at the center gradually flattened with the application from T-5 to T-10, with the temperature at the center decreasing to 33 $^{\circ}\text{C}$ (light purple) for T-10 while at the sides it remains around 30 $^{\circ}$ C (dark purple), indicating an improvement in the distribution of powder at the center and at the sides of the ribbon. The widest flat range in the temperature distribution profile, as seen in T-10, indicates the highest improvement in the uniformity of powder distribution across the ribbon width compared to the other customized guiders. However, when T-14 customized guiders were applied, the temperature distribution profile at the center decreased to 31.5 °C (dark purple) and exhibited non-uniform powder distribution across the ribbons resulting from the over-direction of the high-flowability property of 11SD to the sides, creating friction with the cheek plates.

The shape of the temperature distribution profile in Fig. 19 for 11SD at 60 bar shows significant changes when comparing the selected

customized guiders of T-1, T-4, T-7, and T-14. Initially, the application of T-1 reveals a bell-shaped curve at the center with a temperature around 42 °C (green), while the temperature on the far side of the roller compactor is 32 °C (light purple), and the temperature near the equipment is observed at 35 °C (dark blue). Subsequently, the shape of the curve at the center gradually changes to flat with the application from T-4 to T-7, with the temperature at the center decreasing to 38 °C (blue), and the temperatures on the sides remain around 32 °C (light purple) for both customized guiders. The widest flat range in the temperature distribution profile seen with the application of T-7 indicates the highest improvement in the uniformity of powder distribution across the ribbon width compared to the other customized guiders. However, when T-14 customized guiders were applied, the temperature distribution profile at the center decreases to 32 °C (light purple). This trend exhibits nonuniform powder distribution across the ribbons resulting from the over-direction of 11SD powders with high-flowability property from the center to the sides. The excessive redirection for T-14 led to friction of powders with the cheek plates, generating heat energy which increased the temperature at the sides to be higher than at the center. Moreover, there is a large difference in temperature at the sides of the ribbon, where the temperature on the side far from the roller compactor shows 35 °C (dark blue), while the temperature on the side near the equipment shows 42 $^{\circ}$ C (dark green). The reason for this difference was due to the unidirectional rotation of the screw feeder which drove the 11SD powder with high flowability property more to the side near the body of the roller compactor than the side further from the equipment at high pressure. The friction of a large amount of powder with the rear side cheek plates near the body of the roller compactor has created a large amount of heat energy, significantly increasing the temperature. As for the side far from the roller compactor, some powder was able to escape through the front side cheek plates, reducing the friction of powder with the front side cheek plates and causing the temperature on the side far from the equipment to be lower than the side nearer to the equipment. This can also be seen in Fig. 20 where some of the powders spilled out from the side cheek plates far from the roller compactor with the application of T-14 at 60 bar.

A distinct change in the shape of the temperature distribution profile was observed in Fig. 21 for 11SD at 100 bar when examining the use of the selected customized guiders T-1, T-2, T-7, and T-14. Initially, the application of T-1 shows a bell-shaped curve at the center around 54 °C (medium red). Additionally, the temperature at the side further from the roller compactor is recorded at 46.5 °C (light orange), while the temperature at the side nearer to the body of the equipment is 50.5 °C (light



Fig. 20. Powder leakage from the front side cheek plates.

cheek plates

Y.S. Mohamad et al. Powder Technology 446 (2024) 120158

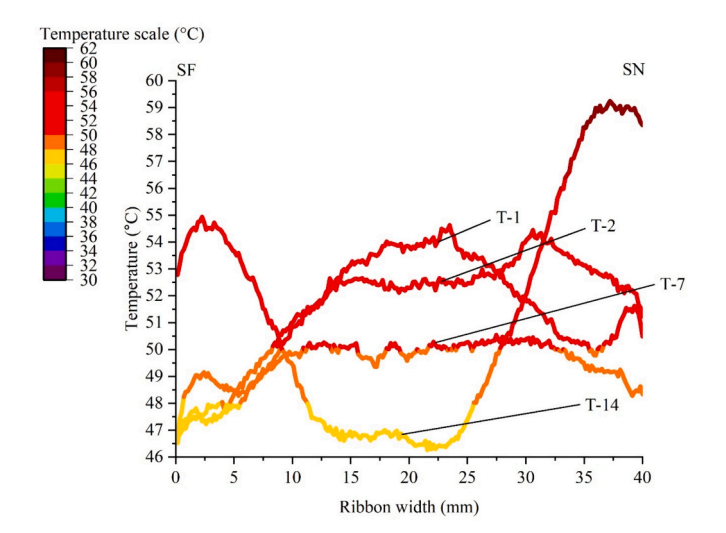


Fig. 21. The temperature distribution profile across the roller width for 11SD powder using selected customized guider at T-1, T-2, T-7 and T-14 at 100 bar.

red). Subsequently, the shape of the curve at the center gradually changes to flat with the application of T-2 until T-7, resulting in a decrease in temperature at the center to around 50 °C (dark orange) and a decrease in temperature at the side near the roller compactor to 48 $^{\circ}$ C (medium orange). This result also highlights that T-7, with a grade of 7 mm, achieved the highest improvement in the uniformity of powder distribution across the ribbon width compared to the other customized guiders at 100 bar. However, when T-14 was applied, the temperature distribution profile at the center dropped to 47 °C (light orange). These results are due to the combined effects of excessive redirection by customized guiders with a 14 mm tip under the influence of the high pressure of 100 bar on high-flowability powder, such as 11SD, pushing the powder from the center to the sides. The excessive redirection for T-14 led to friction of powders with the cheek plates, generating heat energy which increased the temperature at the sides to be higher than at the center. Besides that, the temperature at the far side of the roller compactor for T-14 rose to 53 °C (medium red), while the temperature at the near end of the equipment increased to 59 °C (dark red). The observed difference arises from the unidirectional rotation of the screw feeder, which directs more powder towards the roller compactor's body side than the opposite side under high pressure. Friction between a large amount of powder quantity with the rear side cheek plates generates high heat energy leading to increase in temperature. Conversely, on the far side from the roller compactor, some powder escapes through the front side cheek plates, reducing friction and resulting in lower temperatures compared to the nearer side as shown in Fig. 20.

3.3. Relative temperature uniformity

The relative temperature uniformity was used to determine the uniformity of the ribbon surface temperature starting from the centre to the side of the ribbon. The average relative temperature uniformity of the ribbon produced from Volactose and 11SD powder using different customized guider at 30 bar, 60 bar and 100 bar was presented in Fig. 22 and Fig. 23 respectively.

Fig. 22 shows that at 30 bar, the T-1 and T-2 guiders produced the lowest relative temperature uniformity (23%) for Volactose powders, indicating a non-uniform temperature distribution across the ribbon. The short tips of T-1 and T-2 prevented effective powder redirection, resulting in higher center temperatures. From T-3 to T-14, temperature uniformity increased, with T-14 achieving the highest at 70%, demonstrating effective powder redirection. At 60 bar, relative temperature uniformity gradually increased from T-1 to T-10, peaking at 62% with T-10, about twice that of T-1 (30%). However, T-11 to T-14 showed decreased uniformity, likely due to over-direction of powder, causing non-uniform distribution. At 100 bar, uniformity increased from T-1 to T-8, with T-8 achieving a 60% increase, similar to the 30 bar results. T-8 also produced the widest flat temperature profile. Uniformity declined from T-9 to T-14, indicating non-uniform distribution due to excessive powder redirection.

Fig. 23 shows that for 11SD powders at 30 bar, the application of T-1 to T-5 guiders produced low but gradually increasing relative temperature uniformity. A more consistent increase was observed with T-6 to T-10, indicating improved powder distribution, with T-8 to T-10 achieving the highest uniformity at around 24%. However, as the guider grades increased from 11 mm to 14 mm, uniformity decreased due to overdirection of powder to the sides. At 60 bar, relative temperature uniformity for 11SD powders increased from T-1 to T-7, with guiders between 4 mm and 7 mm showing the widest flat temperature distribution profiles at about 17%. Uniformity decreased with guiders from 8 mm to 14 mm, due to over-direction of powder towards the sides. At 100 bar, uniformity consistently decreased from T-1 (17%) to T-14 (3%). Since relative temperature uniformity measures the length of the uniform temperature section from the temperature profile, starting from the

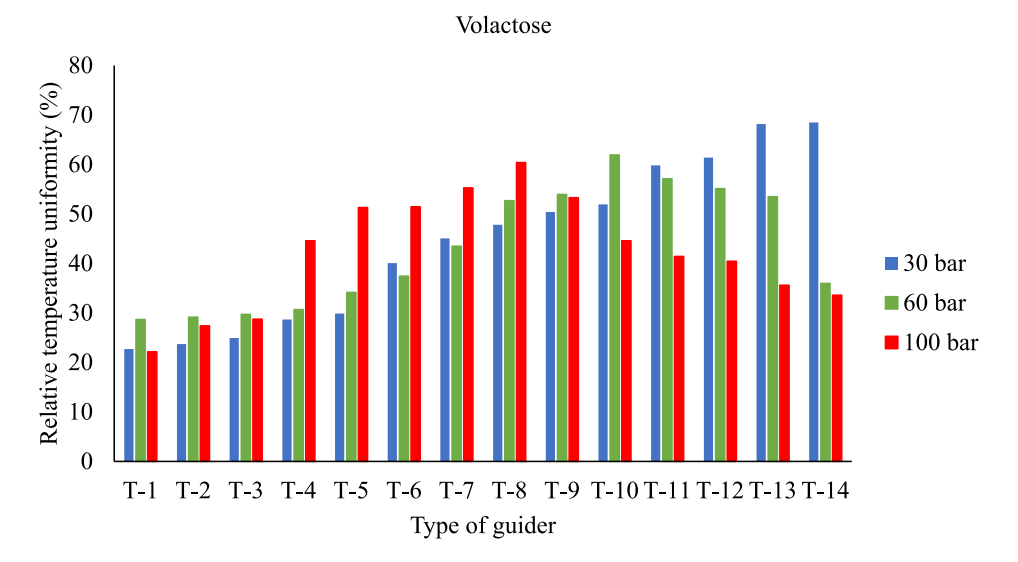


Fig. 22. The relative temperature uniformity of ribbon surface produced from Volactose powders using customized guider T-1 until T-14 at 30 bar, 60 bar and 100 bar.

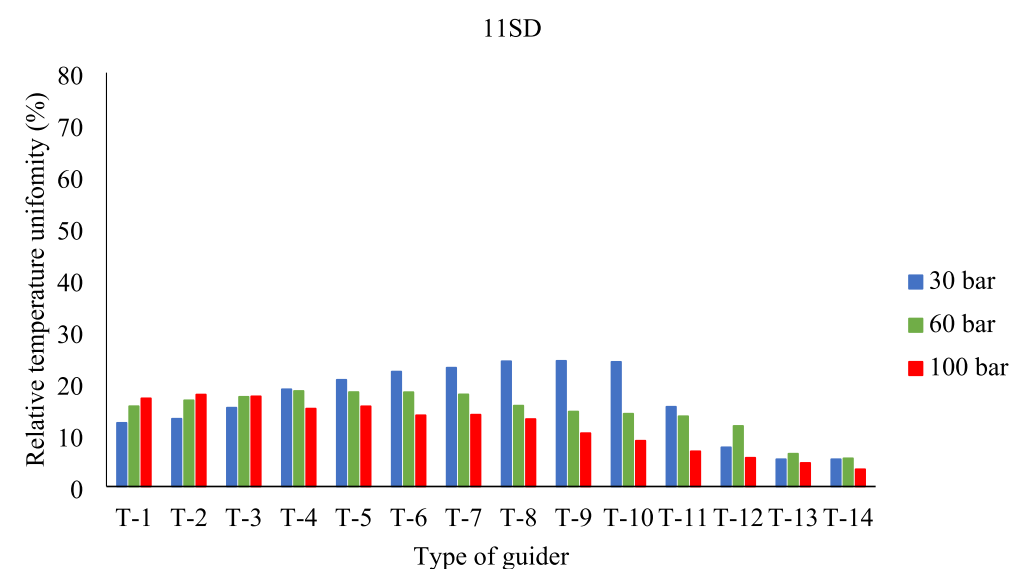


Fig. 23. The relative temperature uniformity of ribbon surface produced from 11SD powders using customized guider T-1 until T-14 at 30 bar, 60 bar and 100 bar.

center to the side, the excessively redirected powder resulting from the application of customized guiders and the high pressure of 100 bar pushed powders to the sides, creating a non-uniform powder distribution across the ribbons and decreasing the percentage of relative temperature uniformity. It is shown from the results from the relative temperature uniformity in both Figs. 16 and 17 show that as the compaction pressure increases, the height of dimension grade for customized guiders resulting in the maximum uniformity decreases.

3.4. Percentage of fines

The amount of fines produced is influenced by the bonding strength among particles during deformation under the roller force. If a smaller quantity of powder is introduced at the sides between the rollers, it will experience less effective compaction in comparison to the powder at the center between the rollers. Consequently, this leads to the formation of weaker areas at the sides of the ribbon. The percentage of fines produced from compacting Volactose and 11SD powders using different customized guider at 30 bar 60 bar and 100 bar was presented in Fig. 24 and Fig. 25 respectively.

At 30 bar, Fig. 24 shows that T-1 exhibited the highest percentage of fines for Volactose at approximately 9.2%, due to insufficient redirection

of powder from the center to the sides, causing uneven stress distribution. As the guider grade increased, the percentage of fines decreased, reaching about 6.5% for T-14, indicating better powder distribution and more uniform stress across the rollers. At 60 bar, the lowest percentage of fines was observed for Volactose when using guiders T-1 to T-10, compared to 30 bar and 100 bar. This was due to the effective combination of powder flowability, guider dimensions, and compacting pressure. Using short guiders at low pressure (30 bar) or long guiders at high pressure (100 bar) led to ineffective redirection and higher fines production. A sudden increase in fines was noted with T-13 and T-14 due to over-direction of powders. At 100 bar, the lowest percentage of fines was achieved with T-1 at approximately 6.6%. As the guider grade increased from T-1 to T-10, a gradual increase in fines was observed due to over-directed powder and leakage under the rollers. A sudden increase in fines was seen with T-11 to T-14, caused by excessive powder redirection leading to leakage and spillage, as shown in Fig. 21. These observations highlight the importance of selecting the appropriate guider dimension based on powder flowability and applied pressure to minimize fines production and ensure uniform powder distribution.

Fig. 25 shows the average percentage of fines produced using customized guiders T-1 to T-14 on 11SD powders at 30 bar. Guiders T-8 to T-10 exhibited the lowest percentage of fines at approximately 5.2%.

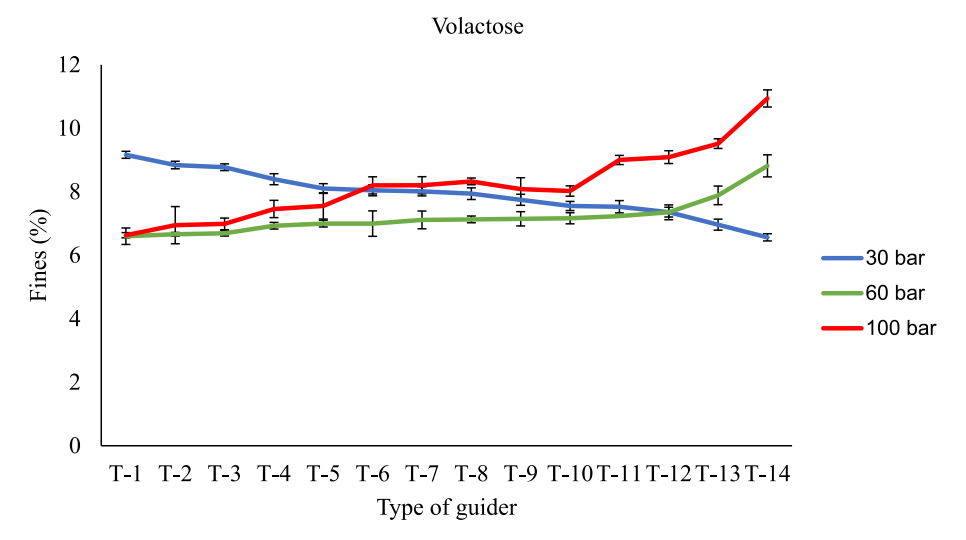


Fig. 24. The percentage of fines produced from Volactose powders using customized guider T-1 until T-14 at 30 bar, 60 bar and 100 bar.

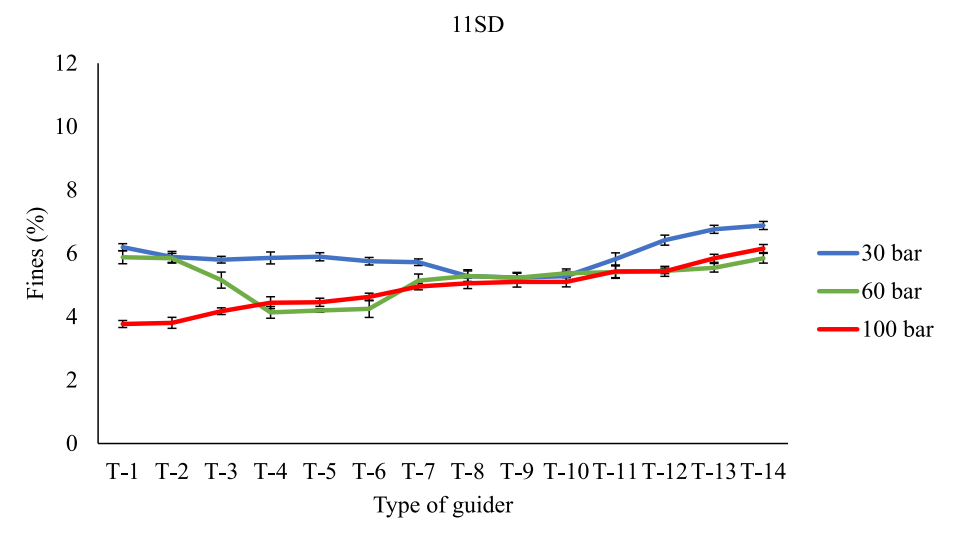


Fig. 25. The percentage of fines produced from 11SD powders using customized guider T-1 until T-14 at 30 bar, 60 bar and 100 bar.

As the grade increased from T-11 to T-14, fines increased from 5.8% to 6.8%, due to over-direction of powder from the center to the sides. At 60 bar, T-4 to T-7 resulted in the lowest fines at about 4.5%, due to more uniform powder distribution. Fines increased suddenly with T-13 and T-14, caused by over-direction and powder leakage under the rollers. This over-direction is evident in Fig. 19, where high temperatures at the sides indicate friction between powder and cheek plates. At 100 bar, fines increased consistently with the guider grade from T-1 to T-14, due to over-direction and powder leakage. However, the fines produced with T-14 were lower than at 30 bar because the higher compaction pressure at 100 bar resulted in stronger ribbons despite the leakage.

3.5. Ribbon width

In roller compactor, despite the roller width used was 40 mm, variations in the width of the produced ribbon were observed across different materials. These variations can be attributed to factors like particle bonding strength and compaction pressure [17]. Additionally, the uneven distribution of powder from feeding to compaction zone also plays a role in influencing the ribbon width. The ribbon width produced from the compaction of Volactose and 11SD at 30 bar, 60 bar and 100

bar was presented in Fig. 26 and Fig. 27 respectively.

Fig. 26 shows that for Volactose at 30 bar, the ribbon width increased from 37.6 mm with T-1 to 39.6 mm with T-14. This indicates that higher guider grades improved powder distribution and stress uniformity during compaction, resulting in wider ribbons. The T-14 guider achieved the highest ribbon width, demonstrating its effectiveness in creating a uniform powder distribution. At 60 bar, ribbon width gradually increased from 37.6 mm with T-1 to 39 mm with T-10. As seen in Fig. 16, T-10 provided the widest and most uniform temperature distribution, enhancing powder distribution and increasing ribbon width. However, ribbon width decreased from T-11 to T-14 due to over-direction of powder, leading to less compaction and narrower ribbons. For Volactose at 100 bar, ribbon width increased from 38 mm with T-1 to approximately 39 mm with T-8. Despite some non-uniform temperature distribution at T-8, as shown in Fig. 17, the 8 mm guider effectively redirected powder, producing the widest ribbons. However, T-9 to T-14 caused over-direction and powder leakage, reducing ribbon width.

Fig. 27 shows the average ribbon width produced from 11SD powders at 30 bar using customized guiders T-1 to T-14. Ribbon width increased from T-1 to T-10, reaching a maximum of approximately 39 mm with T-8 to T-10. A decrease in width was observed with T-11 to T-

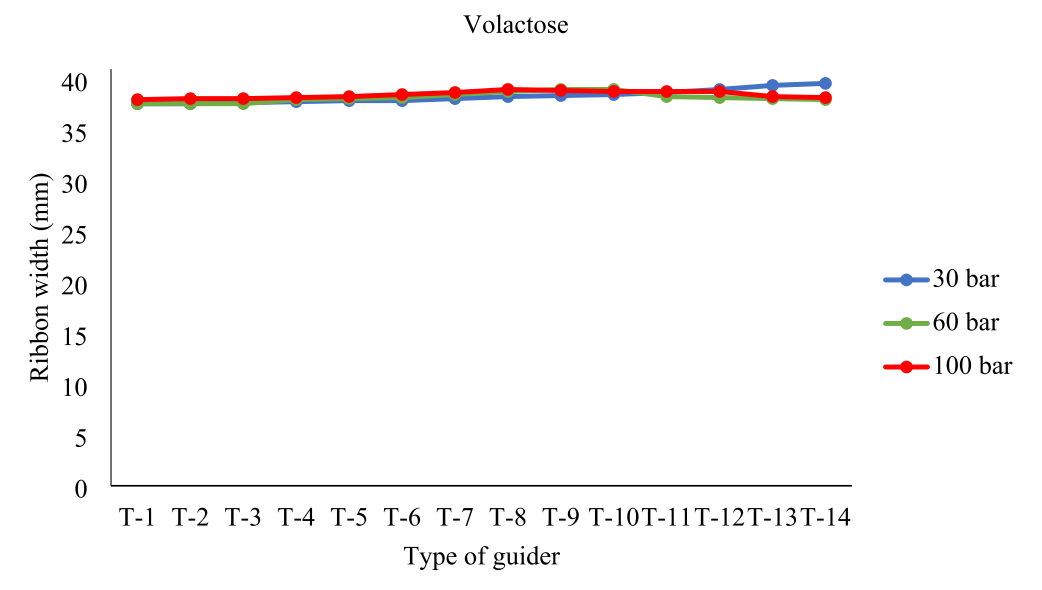


Fig. 26. The ribbon width produced from Volactose powders using customized guider T-1 until T-14 at 30 bar, 60 bar and 100 bar.

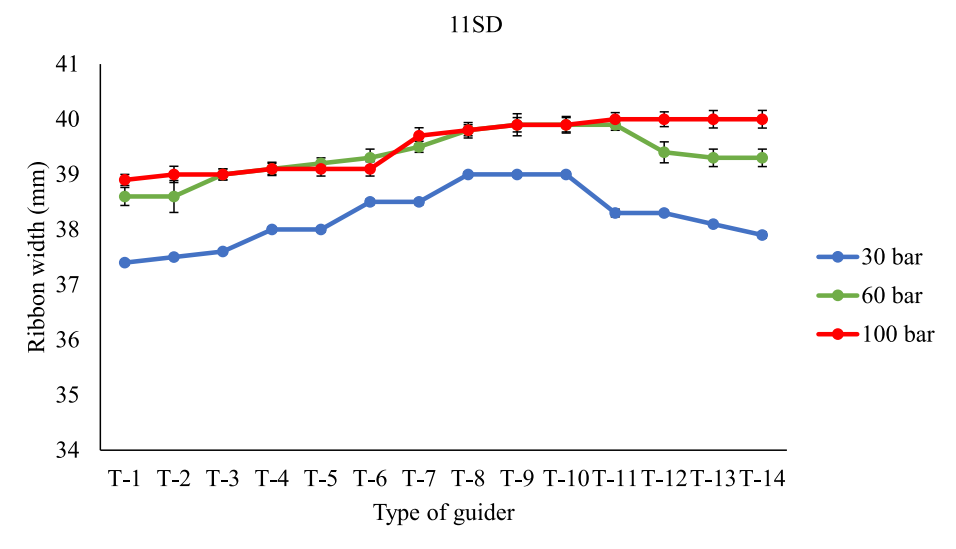


Fig. 27. The ribbon width produced from 11SD powders using customized guider T-1 until T-14 at 30 bar, 60 bar and 100 bar.

14 due to over-direction of powder, resulting in less compaction and powder leakage under the rollers. At 60 bar, ribbon width gradually increased from approximately 38.6 mm with T-1 to 39.9 mm with T-11. The widest ribbons were achieved with T-7 to T-11 guiders, effectively redirecting high-flowability powder to the sides. Ribbon width decreased with T-12 to T-14 due to over-direction and powder leakage. At 100 bar, ribbon width increased from 38.9 mm with T-1, reaching a maximum of 40 mm with T-11 to T-14 guiders. Despite excessive redirection, these guiders effectively redirected the high-flowability powder, resulting in the widest ribbons due to effective compaction.

4. Conclusion

This study aimed to investigate the influence of customized guiders on powder uniformity using online thermal imaging. There are 14 different customized guiders, with dimension grades ranging from 1 mm to 14 mm, were applied to lactose powders with varying flowability at different pressures. Using a thermal camera, the temperature distribution profile across the ribbons was measured, and its relationship with the amount of fines and ribbon width produced was analysed. The results demonstrated that, depending on the powders flowability and compaction pressure, selecting the right guider with optimum dimension grade is crucial for achieving the most uniform powder distribution across the ribbon, minimizing fines production, and maximizing ribbon width. Using a customized guider with a tip that is too short at low pressure proves insufficient for redirecting powder from the center to the sides, resulting in fines being generated from the weaker sides of the ribbons. Conversely, using guiders with excessively long tips at high pressure over-directs the powder, leading to powder leakage from the side cheek plates. These findings suggest that the application of suitable customized guiders can improve powder flow and distribution across the roller width, significantly enhancing product quality and reducing waste during the roller compaction process. This presents a promising prospect for long-term sustainability and resource conservation in industrial applications by reducing the need for material recycling and lowering energy consumption during continuous operations.

CRediT authorship contribution statement

Yang S. Mohamad: Writing – review & editing, Writing – original draft, Visualization, Validation, Project administration, Methodology, Investigation, Funding acquisition, Formal analysis, Data curation, Conceptualization. Mingzhe Yu: Conceptualization. Manfred Felder: Resources. Vincent Meunier: Resources. James Litster:

Conceptualization. Agba D. Salman: Supervision, Conceptualization.

Declaration of competing interest

The authors declare the following financial interests/personal relationships which may be considered as potential competing interests: Yang Sarah Binti Mohamad reports financial support was provided by Council of Trust for the People (MARA). If there are other authors, they declare that they have no known competing financial interests or personal relationships that could have appeared to influence the work reported in this paper.

Data availability

The data that has been used is confidential.

Acknowledgements

We acknowledge the sponsorship from Council of Trust for the People, (MARA), Malaysia. We also acknowledge technical support from Riyadh Al-Asady, University of Sheffield.

References

- P. Guigon, O. Simon, Roll press design—influence of force feed systems on compaction, Powder Technol. 130 (2003) 41–48.
- [2] G. Bindhumadhavan, J.P.K. Seville, M.J. Adams, R.W. Greenwood, S. Fitzpatrick, Roll compaction of a pharmaceutical excipient: experimental validation of rolling theory for granular solids, Chem. Eng. Sci. 60 (2005) 3891–3897.
- [3] A.R. Muliadi, J.D. Litster, C.R. Wassgren, Modeling the powder roll compaction process: comparison of 2-D finite element method and the rolling theory for granular solids (Johanson's model), Powder Technol. 221 (2012) 90–100.
- [4] P. Skikant, J. Akash, D. Mahesh, S. Astik, Roller compaction design and critical parameters in drug formulation and development: review, Int. J. Pharm. Res. Technol. 7 (2015) 90–98.
- [5] C.Y. Wu, W.L. Hung, A.M. Miguelez-Moran, B. Gururajan, J.P. Seville, Roller compaction of moist pharmaceutical powders, Int. J. Pharm. 391 (2010) 90–97.
- [6] R.B. Al Asady, R.M. Dhenge, M.J. Hounslow, A.D. Salman, Roller compactor: determining the nip angle and powder compaction progress by indentation of the pre-compacted body, Powder Technol. 300 (2016) 107–119.
- [7] M. Yu, C. Omar, A. Schmidt, J.D. Litster, A.D. Salman, Roller compaction: infrared thermography as a PAT for monitoring powder flow from feeding to compaction zone. Int. J. Pharm. 578 (2020).
- [8] M. Yu, C. Omar, A. Schmidt, J.D. Litster, A.D. Salman, Improving feeding powder distribution to the compaction zone in the roller compaction, Eur. J. Pharm. Biopharm. 128 (2018) 57–68.
- [9] M. Yu, C. Omar, A. Schmidt, J.D. Litster, A.D. Salman, Application of feeding guiders to improve the powder distribution in the two scales of roller compactors, Int. J. Pharm. 128 (2019) 118815.
- [10] M. Yu, C. Omar, M. Weidemann, A. Schmidt, J.D. Litster, A.D. Salman, Relationship between powder properties and uniformity of ribbon property using feeding guider

- designs with thermography (PAT) in roller compaction, Powder Technol. 128 (2022) 117134.
- [11] M. Becker-Hardt, Continuous Dry Granulation by Roller Compaction: An Introduction to the Alexanderwerk Roller Compaction Process, 2018.
- [12] A.R. Muliadi, J.D. Litster, C.R. Wassgren, Validation of 3-D finite element analysis for predicting the density distribution of roll compacted pharmaceutical powder, Powder Technol. 237 (2013) 386–399.
- [13] A. Michrafy, H. Diarra, J.A. Dodds, M. Michrafy, L. Penazzi, Analysis of strain stress state in roller compaction process, Powder Technol. 208 (2011) 417–422.
- [14] A. Mazor, L. Perez-Gandarillas, A. de Ryck, A. Michrafy, Effect of roll compactor sealing system designs: A finite element analysis, Powder Technol. 289 (2016) 21–30
- [15] L. Perez-Gandarillas, A. Perez-Gago, A. Mazor, P. Kleinebudde, O. Lecoq, A. Michrafy, Effect of roll-compaction and milling conditions on granules and tablet properties, Eur. J. Pharm. Biopharm. 106 (2016) 38–49.
- [16] S. Inghelbrecht, J.P. Remon, Reducing dust and improving granule and tablet quality in the roller compaction process, Int. J. Pharm. 171 (1998) 195–206.
- [17] R.B. Al Asady, M.J. Hounslow, A.D. Salman, Roller compaction: the effect of plastic deformation of primary particles with wide range of mechanical properties, Drug Deliv. Transl. Res. 8 (2018) 1615–1634.
- [18] R.B. Al Asady, M.J. Hounslow, A.D. Salman, Roller compactor: the effect of mechanical properties of primary particles, Int. J. Pharm. 496 (2015) 124–136.
- [19] R. Al-Asady, Roller Compaction: Mechanical Properties of Primary Particles, Pre-Compacted Body and Ribbon, PhD Thesis, University of Sheffield, Sheffield, United Kingdom, 2016.
- [20] M.K. Hwang, S.Y. Kim, T.T. Nguyen, C.H. Cho, E.S. Park, Use of roller compaction and fines recycling process in the preparation of erlotinib hydrochloride tablets, Eur. J. Pharm. Sci. 131 (2019) 99–110.

- [21] C.S. Omar, R.B. Al Asady, A.D. Salman, Roller compaction: improving the homogeneity of ribbon properties along the roller width, Powder Technol. 342 (2019) 464–474.
- [22] J.M. Bultmann, Multiple compaction of microcrystalline cellulose in a roller compactor, Eur. J. Pharm. Biopharm. 54 (2002) 59–64.
- [23] C.C. Sun, P. Kleinebudde, Mini review: mechanisms to the loss of tabletability by dry granulation, Eur. J. Pharm. Biopharm. 106 (2016) 9–14.
- [24] P. Kleinebudde, Roll compaction/dry granulation: pharmaceutical applications, Eur. J. Pharm. Biopharm. 58 (2004) 317–326.
- [25] C.S. Omar, R.M. Dhenge, S. Palzer, M.J. Hounslow, A.D. Salman, Roller compaction: effect of relative humidity of lactose powder, Eur. J. Pharm. Biopharm. 106 (2016) 26–37.
- [26] J.D. Osborne, T. Althaus, L. Forny, G. Niederreiter, M.J. Hounslow, A.D. Salman, Investigating the influence of moisture content and pressure on the bonding mechanisms during roller compaction of an amorphous material, Chem. Eng. Sci. 86 (2013) 61–69.
- [27] L. Fries, J. Dupas, M. Bellamy-Descamps, J.D. Osborne, A.D. Salman, S. Palzer, Bonding regime map for roller compaction of amorphous particles 341 (2018) 51–58.
- [28] C.S. Omar, R.M. Dhenge, J.D. Osborne, T.O. Althaus, S. Palzer, M.J. Hounslow, A. D. Salman, Roller compaction: effect of morphology and amorphous content of lactose powder on product quality, Int. J. Pharm. 496 (2015) 63–74.
- [29] C.S. Omar, M.J. Hounslow, A.D. Salman, Implementation of an online thermal imaging to study the effect of process parameters of roller compactor, Drug Deliv. Transl. Res. 8 (2018) 1604–1614.
- [30] A. Mazor, L. Orefice, A. Michrafy, A. de Ryck, J.G. Khinast, A combined DEM & FEM approach for modelling roll compaction process, Powder Technol. 337 (2018) 3-16